PROCEEDINGS OF SPIE

SPIEDigitalLibrary.org/conference-proceedings-of-spie

Designing 3D-printed LED optics for optimizing target plane application efficacy

Indika Perera, Akila Udage, Nadarajah Narendran, Jean Paul Freyssinier, John Trublowski

Indika U. Perera, Akila S. Udage, Nadarajah Narendran, Jean Paul Freyssinier, John Trublowski, "Designing 3D-printed LED optics for optimizing target plane application efficacy," Proc. SPIE 12216, Novel Optical Systems, Methods, and Applications XXV, 122160K (3 October 2022); doi: 10.1117/12.2633620

SPIE.

Event: SPIE Optical Engineering + Applications, 2022, San Diego, California, United States

Downloaded From: https://www.spiedigitallibrary.org/conference-proceedings-of-spie on 06 Oct 2022 Terms of Use: https://www.spiedigitallibrary.org/terms-of-use

Designing 3D-printed LED optics for optimizing target plane application efficacy

Indika U. Perera[a], Akila S. Udage[a], Nadarajah Narendran[a], Jean Paul Freyssinier[a], and John Trublowski[b]

[a]Lighting Research Center, Rensselaer Polytechnic Institute, 21 Union St., Troy, NY, USA
[b]formerly Eaton Corp., Southfield, MI (retired)

ABSTRACT

At present, solid-state light sources are more efficacious than traditional lighting technologies. To provide benefits in the target applications, this efficacy advantage at the light source has to be supplemented by the optical system used in the lighting system. In general, optical systems can be broadly classified as refractive or reflective based on the optical elements used in the lighting system. Usually, these secondary optic elements are made using injection molding (lenses) or casting and subsequent machining and polishing (reflectors) in large-scale productions. This aspect tends to reduce the use of unique or custom optical solutions in practical applications. Additive manufacturing, or 3D printing, has been successfully used to manufacture small- to medium-scale production volumes of customized solutions in other industries. This technology provides an opportunity to manufacture optical components that maximize the efficacy of a target application by creating unique optical components that facilitate the distribution of light in desired directions. In this study, an optical system based on reflective principles was designed to provide a Type V distribution on the target plane. The designed reflector system was 3D-printed and laboratory tested for total light output, intensity distribution, light output distribution, and optical efficiency. The test results were compared with Monte Carlo ray-tracing simulation results.

Keywords: 3D-printed optics, optical efficiency, application efficacy, beam shaping, lighting, additive manufacturing

1. INTRODUCTION

Light-emitting diode (LED) lighting fixtures and light engines using LED technology have become the preferred lighting source in most lighting applications due to their potential energy efficiency and operational cost savings. The energy-efficient LEDs address energy efficiency at the source or light fixture levels. However, at the application level, the general LED packages with near Lambertian intensity distributions must be combined with secondary optics to tailor the intensity distribution for increased energy efficiency. Studies have shown that uniform illuminance in lighting applications, such as parking lot illumination, could increase the application efficacy and, thus, lower energy use. Furthermore, uniform illumination in lighting applications increases user acceptance due to better visibility and higher perception of safety.[1] Customized secondary optics are required to decrease sudden illuminance variations and maximum-to-minimum illuminance variations on the target plane. This concept of unique customization of optical components is one of the opportunities where 3D printing has the potential to increase U.S. presence in the LED supply chain, as identified by the United States Department of Energy.[2]

This study discussed utilizing a design methodology for creating a custom reflector design, then evaluated the designed and printed reflector and compared it to the designed performance.

Corresponding author: Indika U. Perera
E-mail: pereru2@rpi.edu; Telephone: +1 (518) 687-7133; Website: https://www.lrc.rpi.edu/programs/solidstate/

Novel Optical Systems, Methods, and Applications XXV, edited by Cornelius F. Hahlweg, Joseph R. Mulley, Proc. of SPIE Vol. 12216, 122160K · © 2022 SPIE
0277-786X · doi: 10.1117/12.2633620

Downloaded From: https://www.spiedigitallibrary.org/conference-proceedings-of-spie on 06 Oct 2022
Terms of Use: https://www.spiedigitallibrary.org/terms-of-use

2. METHODOLOGY

This study investigates a method to design a 3D printable first surface reflector device to illuminate an outdoor parking lot lighting application. The project goals predetermined the required type of distribution for the lighting application as a *type V* beam distribution, as defined by the Illumination Engineering Society (IES). For the study, a target distance of 20 ft (~6.1 m) and an illuminance map measuring 40×40 ft^2 (~12.2×12.2 m^2) were selected. This geometry corresponds to the *type V-very short* beam requirements based on IES RP-20-14,[3] and Narendran et al., 2015.[1] The minimum horizontal illuminance level of 5 lx was specified in the IES RP-20-14, and a maximum-to-minimum illuminance ratio of 15:1 was also specified for pre-curfew asphalt surfaces for all zone I.D.s, as per IES RP-20-14. The illuminance values for calculating the maximum-to-minimum illuminance ratio were calculated based on the bin dimensions specified by Narendran et al. (2015).

A single Cree CXB 1830 chip on board (CoB) LED array module with near Lambertian distribution was selected as the light source for the development of the reflector. The LED array module had an intensity distribution of approximately 120° full width at half maximum (FWHM) and approximately 160° full width at one-tenth of maximum (FWTM).

For ray-trace purposes, the target plane distance was transformed to 1.5 m, and dimensions were scaled according to 3.0×3.0 m^2. Similarly, the illuminance requirements were also scaled with the minimum illuminance adjusted to 22.2 lx. The maximum illuminance was scaled to 333.3 lx while adhering to a maximum-to-minimum illuminance of 15:1. The target plane bin dimensions were also scaled to account for the target plane distance, maintaining 16×16 number of bins, with each bin sized at 0.1875×0.1875 m^2.

At the LED package information phase, the identification of the LED source and the source ray information and spectrum information are required from the LED package or module manufacturer. These LED source information files were used to create an apodized source in the Monte Carlo ray-tracing commercial software LightTools™. Figure 1 illustrates the reflector design and evaluation methodology used in this study.

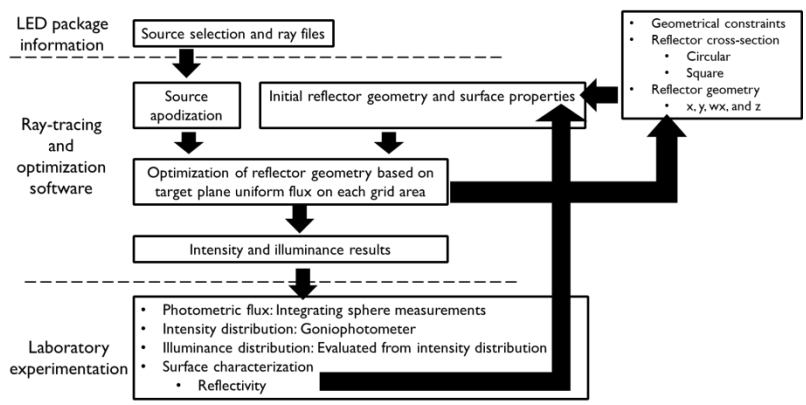

Figure 1. Schematic diagram of the reflector design and evaluation methodology

Initial reflector geometry based on project physical restrictions and limitations was set up in the software CAD modeling step. These limitations include the center hole diameter of 17 mm for the LED source, the maximum reflector aperture diameter of 100 mm, and a maximum reflector height of 50 mm, as illustrated in Figure 2. The reflector cross-sectional shape was also investigated with circular and square cross-section options. The reflector front surface geometry was modeled using a three-point Bezier curve, and the surface reflectance of this front surface was characterized using laboratory experiments. A similar experiment apparatus used by Privitera et al. (2019) was used in the characterization.[4] A surface metallization combined with a post-processing approach and a specular laminate approach were investigated for creating the front surface reflectors.

The generated reflector geometries were then evaluated for total luminous flux, luminous flux on the target, application efficiency, intensity distribution, illuminance on each target plane bin, and maximum-to-minimum illuminance ratio. The reflector parameters were optimized based on these data and each bin's target plane flux

Downloaded From: https://www.spiedigitallibrary.org/conference-proceedings-of-spie on 06 Oct 2022
Terms of Use: https://www.spiedigitallibrary.org/terms-of-use

distribution.[5] These results were compared to the laboratory evaluations of the light engines using an integrating sphere and goniophotometer experiment apparatus.

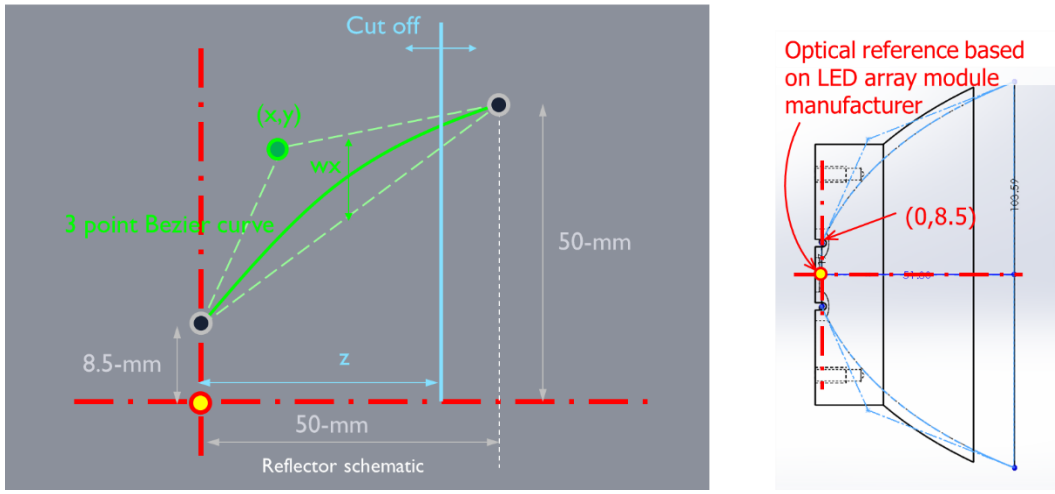

Figure 2. Schematic diagram of the reflector parameters (left) and the optical reference specified by the LED array module manufacturer (right)

The optical reference, indicated by ●, identified by the LED module manufacturer, was used as the origin for the reflector design in a Cartesian coordinate system in this study (Figure 2). Figure 2 also illustrates the coordinates (x, y) of the Bezier curve control point, indicated by ●, relative to the optical reference specified by the LED module manufacturer. The end-points of the Bezier curve, indicated by ●, were fixed based on design constraints introduced by the physical limitations of the project described above and are also noted in Figure 2. Wx represents the weighting of the Bezier curve between a straight line interpolation between the end-points to two straight lines between each end-point and the Bezier curve control point. The cut-off distance from the optical reference along the reflector's optical axis is indicated in z.

Due to the four parameters and their range, an initial parameter analysis was conducted to identify local parameter ranges that would be better investigated using the above-described optimization methodology. Since the parameters x, y, and Wx were all related to the curvature of the reflector, these were used in a parameter analysis, and the resultant application efficiency and maximum-to-minimum illuminance ratio were calculated.[5] The target plane illuminance values were calculated on the 16×16 bins, each bin having dimensions of 0.1875×0.1875 m^2. Table 1 lists the parameters and their respective values used during the parameter analysis.

Table 1. Selected values for parameter analysis

Parameter/variable	P1	P2	P3	P4	P5
***x* [mm]**	0.50	12.75	25.00	37.25	49.50
***y* [mm]**	10.00	20.00	30.00	40.00	50.00
***Wx* [1]**	0.01	0.225	0.50	0.745	0.99
***z* [mm]**	10	20	30	40	50

3. RESULTS

Figure 3 illustrates a selected set of reflector parameter results where the Bezier curve control point coordinates (x, y), the Bezier curve weight (Wx), and the reflector cut-off distance (z) were systematically varied based on the parameter values in Table 1. The application efficiency on the target plane was calculated for the combinations of

Downloaded From: https://www.spiedigitallibrary.org/conference-proceedings-of-spie on 06 Oct 2022
Terms of Use: https://www.spiedigitallibrary.org/terms-of-use

these parameter values. Figure 3 (top) shows the application efficiency as x and y coordinate points are varied for five discrete Wx parameter variables. The chart sequence reveals the application efficiency remained above 90% through the range of x and y variables at Wx values below 0.225. As Wx increased above 0.5, the x and y parameter values along the diagonal produced application efficiencies above 90%. The maximum-to-minimum illuminance ratio of 11.5 was chosen to filter parameter combinations that resulted in high-application efficiency and a high maximum-to-minimum illuminance ratio. Figure 3 (bottom) indicates these parameter combinations in black. Based on these findings, application efficiency higher than 90% and maximum-to-minimum illuminance ratio lower than 11.5 were mainly along the diagonal on x-y space and Wx values ranging from 0.225 to 0.745, indicated by the yellow dashed ellipses in Figure 3 (bottom).

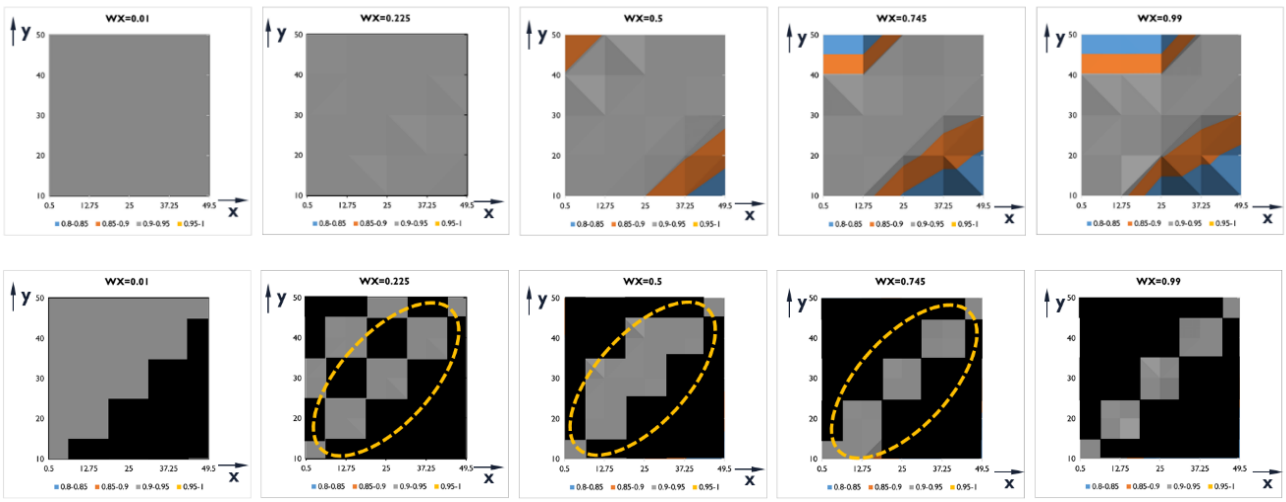

Figure 3. Example results of the parameter analyses at a cut-off variable z=50 mm; application efficiency (top) and application efficiency limited to maximum-to-minimum illuminance ratio <11.5

Table 2. Optimized reflector parameter values

Description	Type of reflector cross-section	x [mm]	y [mm]	Wx [1]	z [mm]
CoB LED module	NA	NA	NA	NA	NA
Reflector A	Circular	12.0	36.4	0.45	40.9
Reflector B	Square	12.0	36.4	0.51	40.9
Reflector C	Square	16.5	36.0	0.56	37.5

Figure 4 shows selected results and the progression of the optimization analyses conducted in LightTools™ ray-tracing software for the narrowed-down parameter ranges. The optimized parameter values are listed in Table 2. Figure 4 (top-left) shows the CoB LED module without any secondary optical system on the target plane 1.5 m away from the source. Only 67% of the flux from the LED CoB source falls within the target area, while the rest of the flux falls beyond the target area.

Downloaded From: https://www.spiedigitallibrary.org/conference-proceedings-of-spie on 06 Oct 2022
Terms of Use: https://www.spiedigitallibrary.org/terms-of-use

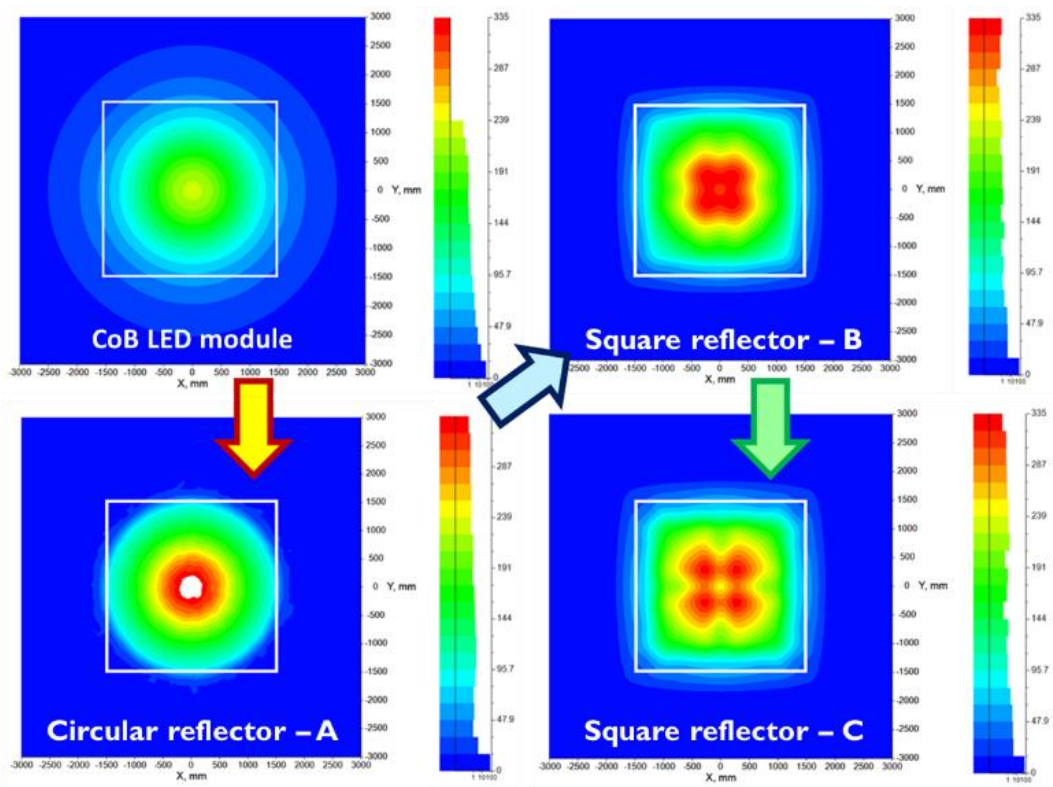

Figure 4. Illustration of reflector parameter optimization transforming the illuminance distribution

The illuminance values were above the specified minimum illuminance ~22 lx and all flux falling within the target generates a higher illuminance in the specified bin array. For the circular reflector – A (bottom-left), with the parameter values listed in Table 2, nearly 90% of the flux emitted by the LED source was directed onto the target area. Due to more flux falling in the center of the target area, increasing the illuminance above the maximum value, and not enough flux falling on the corners of the target area, the application efficiency decreased to 83%, with the illuminance ratio increasing to >75:1. The square reflector – B (top-right) distributed the flux towards the corners of the target area and transformed the illuminance distribution from a circular to a square. This results in the application efficiency increasing to 93% while the maximum illuminance reducing to 331 lx and maintaining an illuminance ratio <15:1. Figure 4 (bottom-right) shows the square reflector – C illuminance distribution. The refinement of the control point and the decreased cut-off point improved the illuminance ratio to 10.2 while maintaining the application efficiency at 93%.

Table 3. Ray-tracing results on the target area of 3.0×3.0 m^2 at a 1.5 m target distance

	CoB LED	Reflector A	Reflector B	Reflector C
Source flux [lm]	1605	1605	1605	1605
Flux on target [lm]	940	1442	1501	1498
Flux on target within the target range of illuminance [lm]	940	1348	1501	1498
Maximum illuminance [lx]*	228	497	331	310
Minimum illuminance [lx]*	24	7	22	30
Max-to-Min Illum. ratio [1]*	9.6	75.3	14.9	10.2
App. Efficiency [1]	67%	84%	93%	93%

* target plane illuminance values calculated on 16×16 bins, each bin having dimensions of 0.1875×0.1875 m^2

Downloaded From: https://www.spiedigitallibrary.org/conference-proceedings-of-spie on 06 Oct 2022
Terms of Use: https://www.spiedigitallibrary.org/terms-of-use

The square reflector – C design was used to manufacture three prototypes, illustrated in Figure 5, using 3D printing. Reflector C-I was 3D printed at Rensselaer Polytechnic Institute with the reflector base on the SLA (stereolithography apparatus) print bed at a layer height of ~25 µm (Figure 5: left). Then the reflector was sent out to a third-party service provider for metallization using electroplating with Ni-Cu coating. Reflector C-II was sent out for 3D printing using an SLA 3D printer and electroplating with Ni-Cu coating by Protolabs Inc. (Figure 5: middle). The layer height was requested to be ~50 µm, although the 3D print orientation was not defined. Reflector C-III was 3D printed using a powder bed fusion 3D printer and post-processed by Eaton Corp. A specular reflective laminate film material was then adhered to the front surface of the reflector to create the specular reflective surface by Eaton Corp. (Figure 5: right).

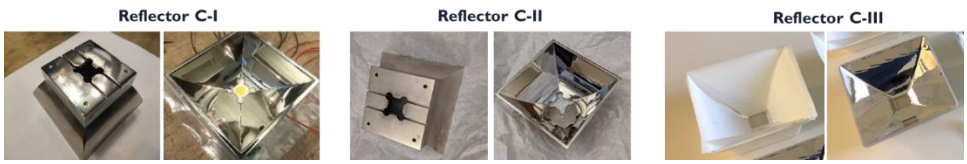

Figure 5. Prototypes of the designed reflector C: Reflector

Figure 6 shows the laboratory-measured intensity distribution (Figure 6: top) and the illuminance distribution calculated from the intensity distribution for a target plane 1.5 m from the reflector aperture (Figure 6: bottom). The intensity distribution is smoother in reflector C-I compared to reflector C-II, indicating the smaller layer height combined with the Ni-Cu plating smoothened out the layer discretization, which might have been the cause of the non-smooth intensity distribution in C-II. The intensity distributions of C-I and C-II are lower than C-III due to the Ni-Cu plating surface reflectance of ~65% compared to ~90% reflectance of the specular laminate film in the wavelength range of 380 to 780 nm. The C-III reflector illuminance calculations from goniophotometer intensity measurements showed similar application efficiency compared to the square reflector C illuminance results from ray-tracing (92% and 93%, respectively). The bins' maximum and minimum illuminance values and the illuminance ratio also showed good agreement between the ray-trace results and calculated values based on goniometer intensity measurements.

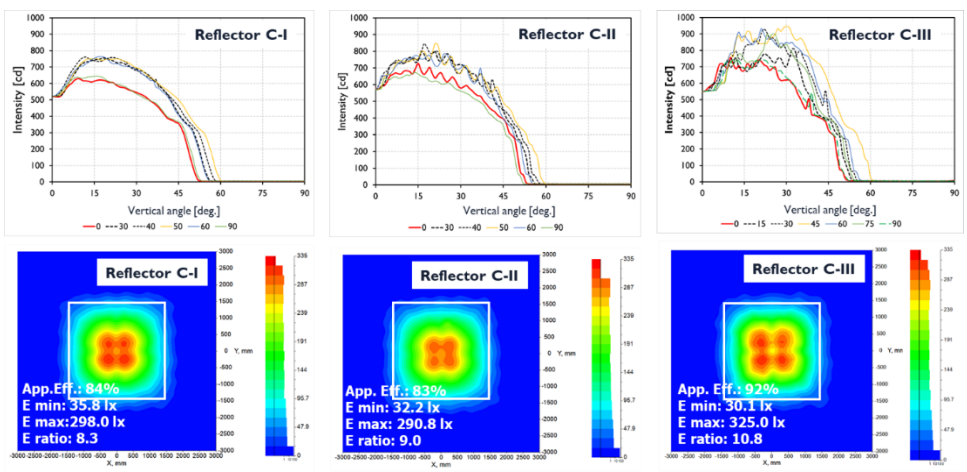

Figure 6. Reflector C intensity distribution (top) and illuminance distribution on target plane 1.5 m from the reflector aperture (bottom)

Due to 3D printing, post-processing, electroplating or laminate adhesion, the square reflector edges could deviate from being square. Ray-tracing was used to check the effect of these edge effects by introducing a constant fillet radius along the edges (Figure 7: top-right) and varying the fillet radii along the edge (Figure 7: bottom-left and bottom-right) and then comparing the results to the original square edge reflector (Figure 7: top=left). The

Downloaded From: https://www.spiedigitallibrary.org/conference-proceedings-of-spie on 06 Oct 2022
Terms of Use: https://www.spiedigitallibrary.org/terms-of-use

modeled reflectors used a surface reflectance of 90% specular (simple mirror type) in these ray-tracing comparions. Ray-tracing results showed the application efficiency was not affected by the edge variations. There were small variations in the illuminance ratio, with the square edge resulting in an 8.5:1 maximum-to-minimum illuminance ratio while the 3 mm constant fillet radius edges resulting in a 8.6:1 maximum-to-minimum illuminance ratio. The most significant variation resulted from the variable edge fillet condition with the fillet radii 3 mm at the base to 12 mm at the reflector aperture.

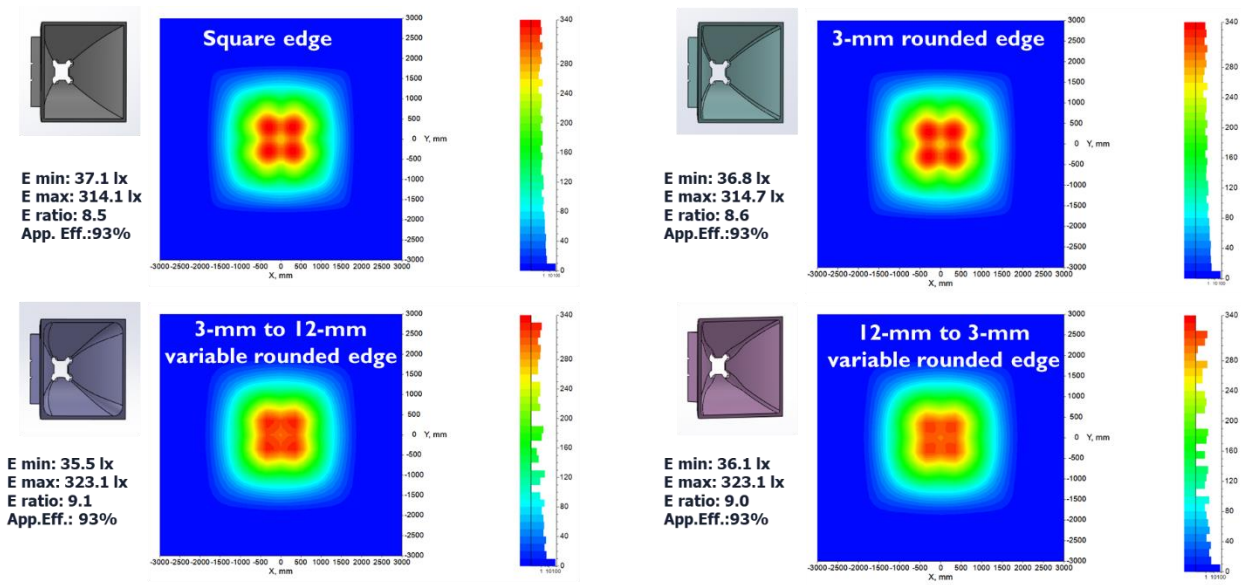

Figure 7. Reflector edge effects on illuminance distribution and application efficiency

4. DISCUSSION

This study proposes using customized parameter-driven reflector geometry and 3D printing to fabricate the designed reflector to redirect light from a light source for increased application efficiency and illuminance uniformity. The study used parameter analysis to decrease the parameter range for successfully optimizing the reflector geometry. Parameter-based design optimization was used to improve the optical performance of the reflector geometry to achieve 93% application efficiency with 7% spillover beyond the target area. The designed reflector achieved a maximum-to-minimum illuminance ratio of 10.2:1. The 3D-printed post-surface metalized reflectors and the 3D-printed with specular laminate film bonded reflector were evaluated for total luminous flux and intensity distribution in the laboratory. The laboratory-measured intensity distributions were used to calculate illuminance distribution on the target plane and compared to the ray-tracing results at the same target plane distance based on the application

All three printed reflectors had 100% coverage, with reflectors C-I and C-II having a better illuminance uniformity (e.g., 8.3:1 and 9.0:1) compared to reflector C-III (10.8:1) due to the lower reflectance of the metalized surface. The specular laminate film bonded reflector, C-III, had a higher application efficiency of 92% compared to the metalized reflectors, C-I and C-II. Ray-tracing results also showed edge effects of the reflector were minimal on the application efficiency and illuminance distribution. The results confirm the possibility of using the 3D-printed reflector design to achieve the prescribed illuminance beam distribution with desired uniformity.

ACKNOWLEDGMENTS

The authors would like to acknowledge the financial support of the U.S. Department of Energy's Office of Energy Efficiency and Renewable Energy (EERE) under the Solid State Lighting Program Award Number DE-EE0008722.

Downloaded From: https://www.spiedigitallibrary.org/conference-proceedings-of-spie on 06 Oct 2022
Terms of Use: https://www.spiedigitallibrary.org/terms-of-use

The authors would also like to thank the assistance of the project team members: Christopher Ring and Nilay Mehta from Eaton Corp.; Jenn Belelie and Ethan Shen from Xerox Research Centre of Canada (XRCC); 3D printing and post-processing of components by Troy Marusich from Protolabs; Jesse Roitenberg and Christopher Wier from Stratasys. The authors also gratefully appreciate Jennifer Taylor from the Lighting Research Center (LRC) for her help in preparing this manuscript and are thankful to Sachintha de Vas Gunawardena of the LRC for his assistance and effort in 3D printing and laboratory measurement. The assistance and support of Groot Gregory and Rhonda Suematsu from Synopsys for the LightTools™ educational license provided to the LRC is acknowledged.

REFERENCES

[1] Narendran, N., Freyssinier, J., and Zhu, Y., "Energy and user acceptability benefits of improved illuminance uniformity in parking lot illumination," *Lighting Research & Technology* 48(7), 789–809 (2016).

[2] U.S. Department of Energy, Office of Energy Efficiency and Renewable Energy, 2020 LED Manufacturing Supply Chain, March 2021. https://www.energy.gov/sites/default/files/2021-05/ssl-2020-led-mfg-supply-chain-mar21.pdf

[3] IESNA RP-20-14 Lighting for Parking Facilities, New York: Illuminating Engineering Society of North America, 2016.

[4] O. Privitera, Y. Liu, I.U. Perera, J.P. Freyssinier, N. Narendran, "Optical properties of 3D printed reflective and transmissive components for use in LED lighting fixture applications," *Proc. SPIE 10940, Light-Emitting Devices, Materials, and Applications, 109401X* (2 April 2019); https://doi.org/10.1117/12.2510063

[5] Synopsys LightTools training material "S3_UniformIntensityLEDLamp" and "S1_ParameterAnalysis"

Downloaded From: https://www.spiedigitallibrary.org/conference-proceedings-of-spie on 06 Oct 2022
Terms of Use: https://www.spiedigitallibrary.org/terms-of-use